

## Research Article

**Cite this article:** Bontovics B *et al.* (2020) The effect of dual inhibition of Ras–MEK–ERK and GSK3 $\beta$  pathways on development of *in vitro* cultured rabbit embryos. *Zygote*. **28**: 183–190. doi: [10.1017/S0967199419000753](https://doi.org/10.1017/S0967199419000753)

Received: 14 April 2019

Revised: 21 September 2019

Accepted: 1 November 2019

First published online: 20 March 2020

**Keywords:**


Blastocyst; Epiblast; GATA6; OCT4; Small molecule inhibition

**Author for correspondence:**

Elen Gócza, NARIC, Agricultural Biotechnology Institute, Animal Biotechnology Department, 2100 Gödöllő, Szent-Györgyi A. str. 4., Hungary  
Tel: +36 28 526 162. Fax: +36 28 526 151.  
E-mail: [gocza.elen@abc.naik.hu](mailto:gocza.elen@abc.naik.hu)

\*These authors contributed equally to this work.

# The effect of dual inhibition of Ras–MEK–ERK and GSK3 $\beta$ pathways on development of *in vitro* cultured rabbit embryos

Babett Bontovics<sup>1,\*</sup>, Pouneh Maraghechi<sup>1,\*</sup>, Bence Lázár<sup>1</sup>, Mahek Anand<sup>1</sup>, Kinga Németh<sup>1,2</sup>, Renáta Fábíán<sup>1</sup>, Jaromír Vašíček<sup>3,4</sup>, Alexander V. Makarevich<sup>3</sup>, Elen Gócza<sup>1</sup>  and Peter Chrenek<sup>3,4,5</sup>

<sup>1</sup>NARIC, Agricultural Biotechnology Institute, Animal Biotechnology Department, 2100 Gödöllő, Szent-Györgyi A. str. 4., Hungary; <sup>2</sup>Department of Laboratory Medicine, Semmelweis University, 1088 Budapest, Szentkirályi str. 46, Hungary; <sup>3</sup>Research Institute for Animal Production Nitra, NPPC, Hlohovecka 2, 951 41 Lužianky, Slovak Republic; <sup>4</sup>Faculty of Biotechnology and Food Science, Slovak University of Agriculture, Hlinku 2, 949 76, Nitra, Slovak Republic and <sup>5</sup>Faculty of Animal Breeding and Biology, UTP University of Science and Technology, Mazowiecka 28, 85-084 Bydgoszcz, Poland

**Summary**

Dual inhibition (2i) of Ras–MEK–ERK and GSK3 $\beta$  pathways enables the derivation of embryo stem cells (ESCs) from refractory mouse strains and, for permissive strains, allows ESC derivation with no external protein factor stimuli involvement. In addition, blocking of ERK signalling in 8-cell-stage mouse embryos leads to ablation of GATA4/6 expression in hypoblasts, suggesting fibroblast growth factor (FGF) dependence of hypoblast formation in the mouse. In human, bovine or porcine embryos, the hypoblast remains unaffected or displays slight-to-moderate reduction in cell number. In this study, we demonstrated that segregation of the hypoblast and the epiblast in rabbit embryos is FGF independent and 2i treatment elicits only a limited reinforcement in favour of OCT4-positive epiblast populations against the GATA4-/6-positive hypoblast population. It has been previously shown that TGF $\beta$ /Activin A inhibition overcomes the pervasive differentiation and inhomogeneity of rat iPSCs, rat ESCs and human iPSCs while prompting them to acquire naïve properties. However, TGF $\beta$ /Activin A inhibition, alone or together with Rho-associated, coiled-coil containing protein kinase (ROCK) inhibition, was not compatible with the viability of rabbit embryos according to the ultrastructural analysis of preimplantation rabbit embryos by electron microscopy. In rabbit models ovulation upon mating allows the precise timing of progression of the pregnancy. It produces several embryos of the desired stage in one pregnancy and a relatively short gestation period, making the rabbit embryo a suitable model to discover the cellular functions and mechanisms of maintenance of pluripotency in embryonic cells and the embryo-derived stem cells of other mammals.

**Introduction**

Rabbit (*Oryctolagus cuniculus*) is potentially a relevant animal model for studying human diseases (Bosze *et al.*, 2003). Several characteristics of rabbit made it the first and classic model for the study of lipoproteins and atherosclerosis. Small rodents do not accurately reflect crucial facets of human cardiovascular physiology, therefore a number of different transgenic rabbit models of hypertrophic cardiomyopathy were created. The scientific community that uses rabbits as experimental animals or as a tool to produce biotech products, as well as those involved in breeding, are invited to focus their efforts on this species (Ivics *et al.*, 2014).

Deriving naïve pluripotent embryonic stem cell lines from rabbit would enable gene targeting for the purpose of modelling human diseases. To this aim, many efforts have been made (Fang *et al.*, 2006; Wang *et al.*, 2007; Honda *et al.*, 2008; Osteil *et al.*, 2013), but the morphology of the colonies and the molecular signature of these cell lines render them more similar to those of primed EpiSCs rather than naïve ESCs typical for mice. Honda *et al.* (2009) reported that bFGF governs the undifferentiated status of rabbit ES cells engaging the Activin/Nodal–Smad2/3 signalling pathway and that they are insensitive to LIF. Furthermore, rabbit inner cell mass (ICM) and epiblasts represent differential expression of genes associated with naïve versus primed pluripotency in mice that proposes differences between mouse and rabbit (Schmaltz-Panneau *et al.*, 2014; Savatier *et al.*, 2017; Taponnier *et al.*, 2017).

Segregation of NANOG-positive epiblast and GATA6-/4-positive hypoblasts (primitive endoderm) is a process that occurs in the blastocyst stage of mouse embryonic development (Plusa *et al.*, 2008), but regulation of this process appears to be species specific.

In human embryos, the GATA4- and SOX17-expressing hypoblast is segregated from the NANOG-expressing epiblast at day 7. After inhibition of FGF, the GATA4-positive hypoblast still forms, indicating FGF-independent formation of the human hypoblast (Kuijk *et al.*, 2012; Roode *et al.*, 2012).

In porcine embryos, NANOG can be first detected at the late blastocyst stage (from day 7.5) (du Puy *et al.*, 2011; Harris *et al.*, 2013). Moreover, the number of ICM cells is not affected, implying that the reduction in GATA4-positive cell numbers was due to partial interference with hypoblast segregation. MEK and GSK3 $\beta$  inhibition and LIF supplementation, which has been used in some studies to impose the naïve state of pluripotency, cannot be used to capture NANOG-positive ICM cells in porcine embryos. Therefore additional signals may be needed to prevent hypoblast formation (Rodriguez *et al.*, 2012).

Transferring the embryonic stem cell derivation technology from mouse to primates (Thomson *et al.*, 1995) and the human system (Thomson *et al.*, 1998) does not yield authentic embryonic stem cell lines. LIF and bone morphogenic protein (BMP4) are required for mouse ESCs to maintain their pluripotent state (Shen and Leder, 1992; Qi *et al.*, 2004; Hao *et al.*, 2006). However, BMP4 induces differentiation of human ESCs (hESCs) (Xu *et al.*, 2002), while basic fibroblast growth factor (bFGF, FGF2) and Activin A promote hESC self-renewal (Vallier *et al.*, 2005; Xu *et al.*, 2005). Mouse ESCs (mESCs) are likely to represent pluripotent stem cells of preimplantation ICM origin, whereas hESCs correspond to a later epiblast stage (Rathjen *et al.*, 1999; Brons *et al.*, 2007; Tesar *et al.*, 2007).

Downstream activation of Ras–ERK signalling by FGFs provided essential stimuli for proliferation and differentiation in many cell types (Thisse and Thisse, 2005). The propagation of ES cells is also enhanced by inhibition of GSK3 (Sato *et al.*, 2004; Ying *et al.*, 2008). A potent inhibitor of MEK, PD0325901 (Bain *et al.*, 2007), can act to achieve suppression of the ERK signalling pathway by preventing its phosphorylation. In combination with an inhibitor of GSK3, CHIR99021 (collectively known as ‘2i’), ES cells can be propagated efficiently and also derived directly from blastocysts of both permissive 129 mouse strains and refractory CBA (agouti coat colour) mouse strains (Ying *et al.*, 2008). First germ line-competent, authentic embryonic stem cell lines from rat blastocysts have also been established using 2i conditioning (Buehr *et al.*, 2008), A-83-01, an inhibitor of type 1 transforming growth factor beta (TGF $\beta$ ) receptor linked to the Activin A/Nodal signalling axis, allowed the cells to grow in relatively homogeneous colonies and contributed extensively to chimerism. A Rho-associated kinase inhibitor, Y-27632, has been found to inhibit apoptosis and increase proliferation, therefore reinforcing survival of hESCs following enzymatic dissociation of colonies into single cells (Watanabe *et al.*, 2007). Based on the above-mentioned findings, Kawamata and Ochiya (2010) combined Y-27632 with CHIR99021, PD0325901 and A-83-01 (termed ‘YPAC’) and successfully established stable and uniform naïve rat ES cells that efficiently contributed to germline chimeras. Latterly, another group succeeded in derivation of a novel germline competent rat ES cell line from Fischer344 transgenic rat using CHIR99021 and PD0325901 (Liskovych *et al.*, 2011; Men and Bryda, 2013).

In present study, we aimed to investigate how different inhibitors, targeting differentiation pathways including Ras–MEK–ERK, GSK3 $\beta$  and TGF $\beta$  signalling pathways, affected the viability and the expression of embryonic stem cell-specific genes in rabbit embryos.

## Materials and methods

### Embryo collection

The animals used were Hycote rabbits handled in compliance with the Hungarian Code of Practice for the Care and Use of Animals for Scientific Purposes. Superovulation and embryo collection were performed as previously published (Besenfelder *et al.*, 1997).

The animals were primed with an intramuscular injection of 120 IU pregnant mare’s serum gonadotropin (PMSG) per animal; 72 h after the PMSG injection, the animals were injected intravenously with 180 IU of hCG per animal and inseminated immediately after the injection. Animals were euthanized for embryo collection, 2-cell-stage embryos were collected after 20 h, 8-cell-stage embryos after 44 h, morula-stage embryos after 68 h, and 5-day-old embryos at 92 h, and 6-day-old embryos at 116 h after insemination. The numbers of collected embryos are shown in Table S1. We collected approximately 40 embryos/female rabbit.

To investigate cell-specific gene expression in trophoblast (TE) and two cell layers of embryoblast: hypoblast (HY) and epiblast (EPI), zona pellucida of 6-day-old embryos at stage 2 were mechanically removed without losing track of the dorsal (epiblast) and ventral (hypoblast) side of the embryonic disc. The embryonic discs (composed of embryoblast cells) were microdissected from the trophoblast under a stereomicroscope, then the embryonic discs were oriented and tungsten needles were used to remove the hypoblasts from the epiblast (Puschel *et al.*, 2010). Isolated hypoblasts, epiblasts and trophoblasts of blastocysts were stored separately at  $-80^{\circ}\text{C}$  until further analysis.

### Embryo culture

The RDH medium was composed of 1:1:1 of RPMI 1640, DMEM and Ham’s F10 medium (Invitrogen, Thermo Fisher Scientific, Waltham, MA, USA) supplemented with 5 mM taurine and 0.3% BSA (both Sigma-Aldrich, St Louis, MO, USA). RDH medium was used to prepare 2i, 3i and 4i supplemented medium. The inhibitors were first reconstituted as 1 mM stock solutions, prepared in dimethyl sulfoxide. Stock solutions were stored at  $-20^{\circ}\text{C}$  until use.

The final concentrations of inhibitors in RDH medium were as follows: 2i: 1  $\mu\text{M}$  of PD0325901, 3  $\mu\text{M}$  of CHIR99021 (04-0004, StemGent, Cambridge, MA, USA); 3i: 1  $\mu\text{M}$  of PD0325901, 3  $\mu\text{M}$  of CHIR99021, 10  $\mu\text{M}$  of Y-27632 (04-0012, StemGent); 4i: 1  $\mu\text{M}$  of PD0325901, 3  $\mu\text{M}$  of CHIR99021, 10  $\mu\text{M}$  of Y-27632, 0.5  $\mu\text{M}$  of A-83-01 (0-0014, StemGent).

All rabbit embryos were cultured in RDH, 2i, 3i or 4i medium covered by embryo-tested light paraffin oil (Sigma-Aldrich) at  $38.5^{\circ}\text{C}$  under 5%  $\text{CO}_2$  in humidified air (Jin *et al.*, 2000).

### Immunohistochemistry

Immunostaining of embryos was performed using primary antibodies against OCT4 (ab27985, 1:100; Abcam, Cambridge, UK), CDX2 (ab15258, 1:100; Abcam), GATA6 (AF1700, 1:10; R&D Systems Europe, UK). Secondary fluorochrome-conjugated antibodies (Jackson ImmunoResearch Laboratories, West Grove, PA, USA) were diluted 1:400 in blocking buffer. Nuclear staining was performed by embedding the samples into DAPI containing Vectashield mounting medium (H-1200; Vector Laboratories, Burlingame, CA, USA). Embryos and embryo outgrowths were fixed in 4% paraformaldehyde, for 10 min at room temperature. The cells were permeabilized and blocked in one step using PBS

with 0.5% Triton X-100 and 3% BSA. Cells were incubated with primary antibodies overnight at 4 °C, thoroughly washed and then incubated with the secondary antibodies at 37 °C for 1 h prior to final washing and mounting in Vectashield mounting medium (H-1200, Vector Laboratories) with DAPI onto microslides. Samples were visualized using a Carl Zeiss Axio Imager 2 fluorescence microscope and a Carl Zeiss LSM 700 confocal microscope (Carl Zeiss AG, Oberkochen, Germany).

### Transmission electron microscopy

Rabbit embryos were fixed in the aldehyde mixture (2.5% glutaraldehyde and 2% paraformaldehyde in 0.15 M cacodylate buffer, pH 7.1–7.3) for 1 h at 4 °C, and washed twice in a cacodylate buffer, 5 min each. The individual embryos were embedded into 4% agar and post-fixed in 1% osmic acid in cacodylate for 1 h. Samples were dehydrated in a series of progressively concentrated ethanol solutions and mounted into Durcupan ACM (Fluka, Sigma-Aldrich). Semithin sections (1–2 µm) were stained with methylene blue. Ultrathin sections (75–90 nm) were placed on copper or nickel meshes and were contrasted with lead uranyl acetate and lead citrate. Electron micrographs for morphometric measurements were acquired using a transmission electron microscope JEM 100 CX II (JEOL, Tokyo, Japan) at an acceleration voltage of 80 kV. Finally, 10 or 11 electron micrographs were made out of each embryo and analyzed at ×7200 magnification.

Relative volume (%) of cell organelles was determined using a method published earlier (Bolender and Weibel, 1973). Line segments with 150 test points were placed on each micrograph. The number of test points, within the area of the analyzed organelle, was divided by the total number of points in the line segments, and the resulting value was expressed in per cent. The volume of the individual organelles per sample was calculated based on the sum of all values measured from the individual micrographs. The organelles analyzed in this way included: mitochondria (M), endoplasmic reticulum (ER), Golgi complex (GC), vacuoles (V), residual bodies (RB) and apoptotic bodies (AB).

Statistical significance of the difference in volume was determined using the chi-squared ( $\chi^2$ ) test. The difference was considered to be significant at a  $P$ -value = 0.05. Statistical analyses of the individual organelle volumes were carried out using Student's  $t$ -test.

### Real-time quantitative polymerase chain reaction (PCR)

Total RNA was extracted from rabbit embryos using TRIzol reagent (Invitrogen, Thermo Fisher Scientific) according to the manufacturer's instructions. RNA was then reverse transcribed into single-stranded cDNA, using a High Capacity cDNA Reverse Transcription Kit (Applied Biosystem, Foster City, CA, USA). Synthesized cDNA templates were subjected to quantitative real-time PCR analysis using the SYBR® Green PCR Master Mix, with rabbit-specific primer sets to *OCT4*, *GATA6* and *CDX2* genes (Maraghechi *et al.*, 2013). All reactions were performed in an Eppendorf Mastercycler RealPlex<sup>4</sup>. Relative mRNA levels were calculated using the comparative  $C_T$  method ( $\Delta\Delta C_T$  method) and normalized to GAPDH. For each sample, the signal was averaged over replicates. Each biological replicates of embryos consisted of a pool of staged embryos and isolated hypoblasts, epiblasts and trophoblasts.

### Statistical analysis

All data were analyzed using GenEx (version 6.0), and a  $P$ -value < 0.05 was considered to be significant (\* $P$  < 0.05, \*\* $P$  < 0.01, \*\*\* $P$  < 0.001).

Statistical differences were assessed using one-way analysis of variance (ANOVA) and GenEx 6.0 software. Comparisons between the mean values of the control group and those of each experimental group were performed using Tukey's post hoc test for multiple comparisons.

## Results

### Pluripotency and early differentiation marker expression in 4-day-, 5-day- and 6-day-old embryos

To investigate the baseline expression of different embryonic stem cell-specific markers, 4-, 5- and 6-day-old rabbit embryos, recovered from the uterus, were immunostained with antibodies specific for the pluripotent stem cell marker OCT4 and an early differentiation/hypoblast marker GATA6. In 4-day-old embryos, we detected OCT4 expression only in a few nuclei. In 5-day-old embryos, OCT4 expression started to localize in most of the nuclei of embryoblast (EB). On day 6, OCT4 expression became exclusive to the cells of the embryoblast (Fig. 1A). GATA6 expression in 4-day-old embryos was limited to the trophoblast (TE) with varying intensities among the individual cells. The same expression pattern for GATA6 was observed in 5-day-old embryos. In 6-day-old embryos, GATA6 was expressed in the embryoblast as well as in trophoblast with varying intensities. However, based on GATA6 expression in 6-day-old embryos, epiblast and hypoblast and boundaries between the ICM and trophoblast were indistinguishable from each other upon analyzing the confocal images (Fig. 1B).

We further analyzed GATA6 and CDX2 co-expression in 6-day-old embryos (Fig. 1C1, C2). In the trophoblast layer, most of the cells were CDX2 positive (green circle), but we also detected CDX2 and GATA6 double-positive (yellow circles) and double-negative (blue circles) cells. In the embryoblast we found both GATA6-positive (red circles) and GATA6-negative cells.

To delineate the transcription levels of OCT4, GATA6 and CDX2, we performed quantitative real-time PCR analysis on day 4 (Fig. 1D) and day 6 (Fig. 1E) *in vivo* developed rabbit embryos. We detected high expression levels of *OCT4*, *GATA6* and *CDX2* transcripts on day 4. To get a more comprehensive profile of cell-specific gene expression we further analyzed the expression of *OCT4*, *GATA6* and *CDX2* in trophoblast (TE) and two cell layers of the embryoblast: the hypoblast (HY) and epiblast (EPI) of day 6 embryos using real-time quantitative PCR. We detected significantly high expression levels of *OCT4* in the epiblast compared with the hypoblast and trophoblast (Fig. 1E). *GATA6* expression was higher both in the hypoblast and trophoblast (Fig. 1E). *CDX2* expression was restricted to the trophoblast both at the transcriptional (Fig. 1E) and protein level detected by confocal microscopy (Fig. 1C1, C2).

### Effect of 2i, 3i and 4i conditions on *in vitro* development of rabbit embryos

Next, we studied the effect of inhibitors on different pathways in rabbit embryo development and how they preserve their viability over the culture period. The inhibitors used were as follows:



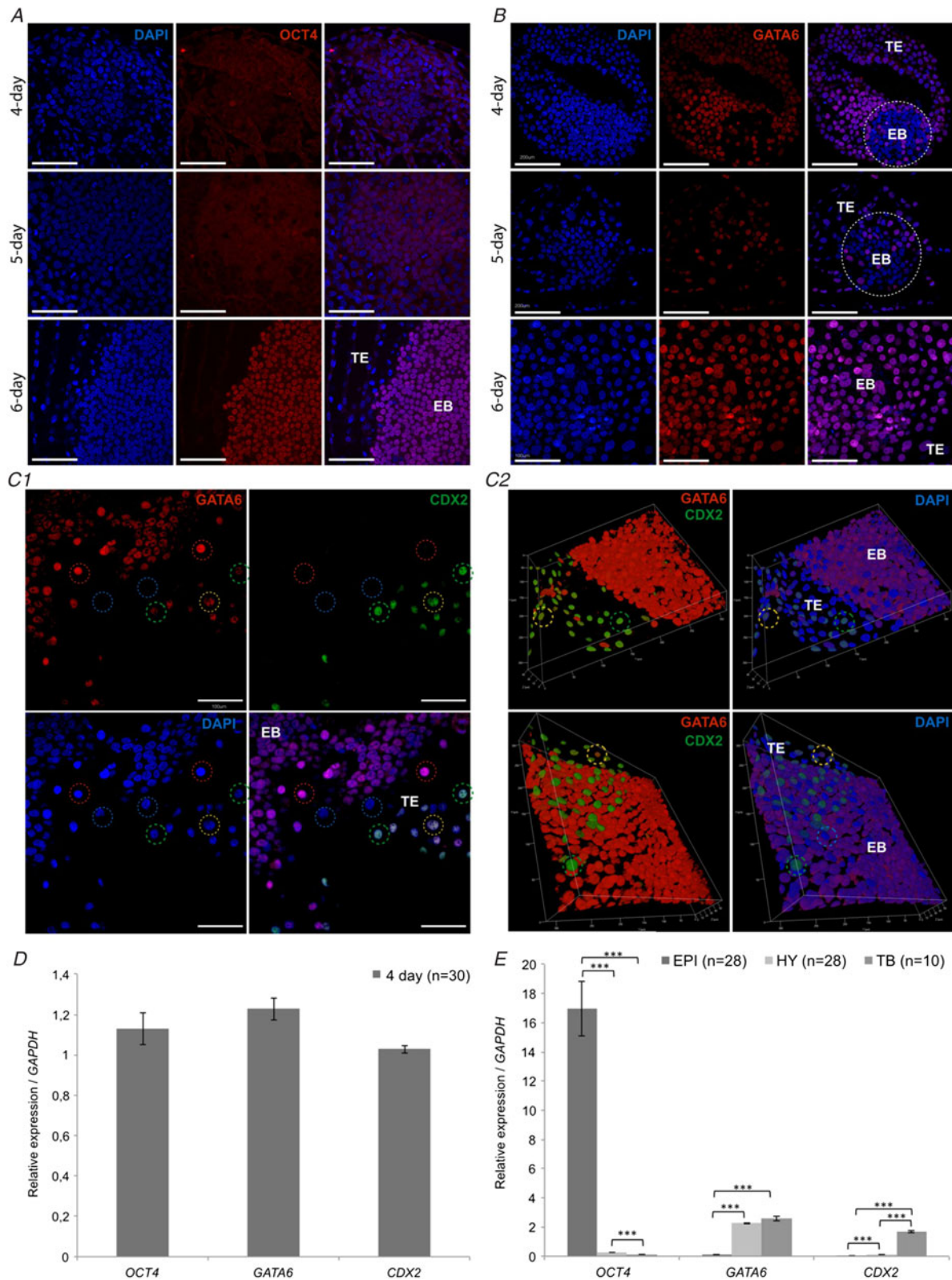


**Figure 1.** Expression of pluripotency and early differentiation markers in rabbit blastocysts. (A) Baseline expression of *OCT4* in rabbit embryos after their recovery from oviducts on days 4 and 5, and from the uterus 6 days after insemination. *OCT4* expression was fully developed on day 6. (B) Baseline expression of *GATA6* in embryos after their recovery on days 4, 5 and 6 after insemination. *GATA6* expression was limited to non-ICM cells in 4-day- and 5-day-old embryos. In 6-day-old embryos, *GATA6* expression was observed in both ICM and non-ICM cells at varying intensities. Scale bars: 200  $\mu$ m, 100  $\mu$ m. (C) *GATA6* and *CDX2* co-expression in 6-day-old embryos showed that most of the trophoblast cells (top row) were *CDX2*-positive (green dotted circle), *CDX2*/*GATA6* double-positive cells (yellow dotted circles) and *CDX2*/*GATA6* double-negative cells (blue dotted circles) were also detected; the embryoblast (bottom row) was comprised *GATA6*-positive cells (red dotted circles) and *GATA6*-negative cells (blue dotted circles). Scale bars: 100  $\mu$ m. (C2) Confocal 3D reconstructions of (C1) images showing the interface of trophoblast (TE) and embryoblast (EB). (D, E) Quantitative expression of *OCT4*, *GATA6* and *CDX2* mRNAs in 4-day-old (D) and 6-day-old (E) rabbit embryos. High levels of expression of *OCT4*, *GATA6* and *CDX2* transcripts were detected by day 4 of embryonic development. Epiblast of day-6 embryos expressed *OCT4* in significantly high levels compared with the hypoblast and trophoblast. *GATA6* was expressed at almost equal level in trophoblasts and in hypoblasts and downregulated in epiblasts, while *CDX2* expression was limited to trophoblasts. Expression levels were calculated relative to the 7-day mRNA level and normalized to the *GAPDH* transcript level. Error bars indicate  $\pm$  standard deviation (SD) (\*\*\* $P \leq 0.001$ ),  $n$  = number of investigated embryos.

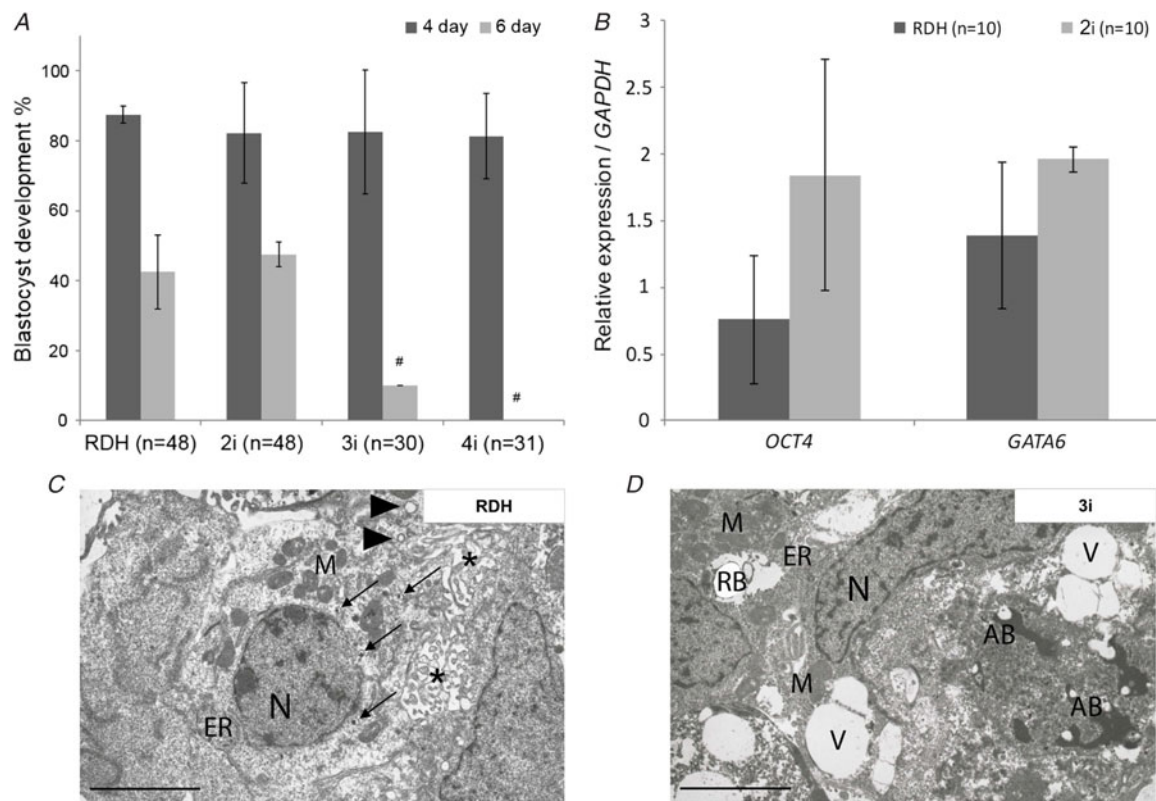


**Figure 2.** *In vitro* development of rabbit embryos under 2i, 3i or 4i conditions. (A) Percentage of *in vitro* cultured embryos (devoid of zona pellucida) from the 8-cell stage that successfully developed to the compact morula stage on day 4 after insemination (dark grey lines) compared with the control RDH-cultured embryos. Percentage of the same embryos after continued culture that successfully developed to the expanded blastocyst stage on the day 6 after insemination (light grey lines). 3i and 4i treatments resulted in the death of the embryos. Error bars indicate  $\pm$  SD ( $*P \leq 0.05$ ). (B) Quantitative real-time PCR analysis showing the expression of *OCT4* and *GATA6* in 6-day-old embryos cultured from the 8-cell stage in 2i or the control RDH medium. The highest expression of *OCT4* transcript was detected under 2i conditions. (C, D) Transmission electron micrographs of the ICM of the 6-day-old embryos cultured under control RDH or 3i conditions. The figures depict healthy organelles (RDH) and damage arising from the culture conditions that does not support viability of the embryos (3i). The electron micrograph shows three cells of the ICM from the control group of embryos in RDH. One of these was localized to the centre of the image with the oval nucleus (N) and nucleoli localized in the centre of the cytoplasm. Intercellular spaces are partially extended (\*). The electron micrograph of two cells of the ICM of rabbit embryos treated with 3i shows numerous large oval vacuoles (V), residual bodies (RB) and apoptotic bodies (AB) located in the vicinity of an elongated nucleus (N) of the heterochromatic type. The presence of mitochondria (M) and granular ER is very rare. Individual structures: mitochondria (M) (dark and oval); granular ER; small residual bodies ( $\rightarrow$ ); and small vacuoles ( $\blacktriangleright$ ) around the ESC. Magnification:  $\times 7200$ . Scale bars: 5  $\mu$ m;  $n$  = number of investigated embryos.

PD0325901 for MEK/ERK, CHIR99021 for GSK3 $\beta$ , A-83-01 for TGF $\beta$  receptor and Y27632 for ROCK. The following treatment groups based on the combinations of these inhibitors were: PD0325901 and CHIR99021 (2i); PD0325901 plus CHIR99021 and Y27632 (3i); and PD0325901 plus CHIR99021 plus A8301 and Y27632 (4i).

We started by observing how the inhibition of the respective pathways affected viability of the embryos. The percentage of *in vitro* cultured embryos (devoid of zona pellucida) from the 8-cell stage that successfully develop to the early blastocyst stage, 4 days after insemination did not differ across the treatment groups of 2i (82.2%), 3i (82.5%) and 4i (81.4%) compared with the control RDH-cultured (87.5%) embryos (Fig. 2A). Continued culture of the same embryos up to day 6 *post coitum* expanded blastocyst revealed tolerance of the embryos to 2i (47.5%) conditions; the percentage of embryos that successfully developed to the expanded blastocyst was comparable with the percentage observed in the control RDH-cultured embryos (42.5%). Under 3i conditions we noticed 10% of expanded blastocysts, but for 4i (0%) treatments no expanded blastocysts were observed (Fig. 2A).

Moreover, we performed real-time quantitative PCR analysis to investigate the effect of inhibitors on the expression of pluripotency-associated marker *OCT4*, and an early differentiation

marker *GATA6* in 6-day-old rabbit embryos cultured from the 8-cell stage in inhibitor-supplemented medium (Fig. 2B), compared with the control embryos cultured in RDH medium with no inhibitors. The best performing condition appeared to be 2i, as the transcription levels of pluripotent marker, *OCT4*, were 2.4-fold higher compared with the control embryos cultured in RDH with no inhibitors (Fig. 2B). In contrast, transcription of *GATA6* in embryos treated with 2i did not display substantial increase compared with the control embryos in RDH (Fig. 2B).

To find a reason for embryo development arrest, the integrity of the cells and their organelles in rabbit embryos cultured under individual inhibition culture conditions was analyzed using transmission electron microscopy (Fig. 2C, D). We measured the relative volume (%) of the cell organelles in the ICM of the 6-day-old embryos cultured under 2i, 3i and 4i conditions (Table 1). It was found that the mitochondria (M; 7.5%), the endoplasmic reticulum (ER; 9.7%) and the Golgi complex (GC; 3.4%) were significantly larger in the control group (Table 1 and Fig. 2C) compared with 3i conditions (M, 5.2%, ER, 4.7%, and GC, 2.8%; Table 1 and Fig. 2D) and 4i condition (M, 1.9%, ER, 4.5%, and GC, 1.7%; Table 1). The difference in relative volume of these organelles between the control and 2i was not significant, indicating that the 2i conditions were safe for organelle integrity (Table 1). *In vitro* culture of embryos in medium supplemented with

**Table 1.** Relative volume (%) of organelles in the ICM cells of 6-day-old rabbit embryos cultured in inhibitor-supplemented medium

	RDH (n = 10)	2i (n = 10)	3i (n = 11)	4i (n = 10)
Mitochondria (M)	7.50 <sup>a</sup>	6.67	5.15 <sup>b</sup>	1.93 <sup>b</sup>
Endoplasmic reticulum (ER)	9.67 <sup>a</sup>	6.87	4.73 <sup>b</sup>	4.53 <sup>b</sup>
Golgi complex (GC)	3.40 <sup>a</sup>	2.87	2.78	1.73 <sup>b</sup>
Vacuoles (V)	4.87 <sup>a</sup>	6.2	6.18	7.20 <sup>b</sup>
Residual bodies (RB)	5.13 <sup>a</sup>	9.73 <sup>b</sup>	14.12 <sup>c</sup>	16.73 <sup>c</sup>
Apoptotic bodies (AB)	0.40 <sup>a</sup>	0.4	2.20 <sup>b</sup>	0.6

<sup>a</sup>vs. <sup>b</sup> significant difference at  $P < 0.05$ ;

<sup>a</sup>vs. <sup>c</sup>  $P < 0.01$ ; n = number of investigated embryos.

4i resulted in a significant increase in the size of the vacuoles (7.2% versus 4.9% in the control; Table 1). The relative volume of the RBs in embryo cells was significantly higher in all of the inhibitor-supplemented medium: 9.7% in 2i, 14.1% in 3i, 16.7% in 4i versus 5.1% in the control medium (Table 1). The relative volume of ABs in 3i-supplemented medium was significantly higher (2.2%) compared with control medium (0.4%), while in 4i-supplemented medium there was no significant difference compared with the control (Table 1).

In accordance with the results obtained from confocal microscopy, quantitative real-time PCR analysis and electron microscopy morphometry, we proposed that addition of 2i gave the best conditions in which to keep the undifferentiated state of the pluripotent cells in the rabbit embryo.

#### Rabbit early embryonic development in RDH and 2i conditions followed by time-lapse microscopy

Subsequently, we tracked embryonic development in control culture condition (RDH) against 2i-supplemented culture medium using time-lapse video technology to measure the time between the different embryonic developmental stages, from the 2-cell stage up to the early blastocyst stage (75 h). For the embryonic developmental rate in 2i-supplemented medium and in the control RDH medium we could not detect significant differences (Fig. 3A). Similar effects were observed in another time-lapse video experiment comparing the development of the embryo in control contrasted with the 2i culture conditions from the morula up to the blastocyst stage over the span of 48 h. The difference in size of the embryos cultured in control and 2i conditions was not significant (Fig. 3B). According to these findings we can conclude that 2i treatment did not significantly affect the development of the rabbit embryos from the 2-cell stage up to the early blastocyst stage (Movie S1).

#### Discussion

ESCs are sustained by a flexible signalling and transcription factor network that appears to be closely related to the network existing in the embryo. The notion of naïve pluripotency implies that early epiblast cells and their counterpart ESC derivatives have equal unrestricted access to all somatic lineages and the germ line (Nichols and Smith, 2011).

To examine the expression of transcription factors in rabbit embryos, epiblasts, hypoblasts and trophoblasts, we first analyzed the transcription patterns of *OCT4*, *GATA6* and *CDX2* genes in rabbit embryos recovered at consecutive developmental stages. Real-time quantitative PCR results clearly showed the difference

in the expression patterns of *OCT4*, *GATA6* and *CDX2* transcripts. In epiblast cells *OCT4* transcripts were expressed at significantly high levels, and underlines the pluripotent status of these cells. *CDX2* expression was significantly higher in trophoblast cells than in other layers; this was consistent with trophoblast specificity of *CDX2*. *GATA6* was expressed in almost equal levels in trophoblast and in hypoblast cells and downregulated in epiblast cells.

We investigated how *OCT4* and *GATA6* are normally expressed in *in vivo* developed embryos recovered from uteri at 4, 5 and 6 days after insemination. Expression of the pluripotency marker *OCT4* was first detected exclusively in the nuclei of cells of the embryoblast in 6-day-old embryos. *GATA6* expression in 4- and 5-day-old embryos was limited to non-ICM cells, but in 6-day-old embryos its expression was observed in all cells of the embryo. The embryoblast was comprised of *GATA6*-positive and *GATA6*-negative cells, while some cells of the trophoblast exhibited *GATA6* signal. However, the majority of the trophoblast cells were only *CDX2*-positive. In rabbit embryos, downregulation of *GATA6* in a subset of ICM cells appeared to occur independently of *NANOG*. *NANOG* is present in the nuclei of both *GATA6*-negative and *GATA6*-positive cells at the early blastocysts stage, as was published by Piliszek et al. (2017).

In our following experiments, we tested how different combinations of inhibitors of early differentiation pathways affect the development, transcription and expression of *OCT4* and *GATA6*. The effect of the Ras-MEK-ERK1/2 blockade on development of preimplantation embryos has been investigated in different species. PD0325901 is a very selective inhibitor of the MEK/ERK pathway (Lorusso et al., 2005; Haura et al., 2010; Sheth et al., 2011). CHIR99021 is an inhibitor of the GSK3 pathway. These two inhibitors are collectively named '2i' (Ying et al., 2008). According to our time-lapse video analysis, the embryos in 2i-supplemented culture condition developed normally. Similarly, quantitative real-time PCR analysis of rabbit embryos revealed that under 2i conditions transcription of *GATA6* and *OCT4* is present. Similar to our findings, Piliszek et al. (2017) did not observe any increase in the number of SOX2-positive EPI cells in rabbit embryos treated with 2i inhibitor in comparison with control embryos. This result suggested that blocking FGF signalling was not sufficient alone, and that an additional signal was required in rabbit (Piliszek et al., 2017). In mouse 8-cell-stage embryos, the blockade of ERK signalling completely abolished the development of hypoblast cells (Nichols et al., 2009). In species other than mice or rat, MEK inhibition does not result in ablation of hypoblast cells in the ICM of the blastocysts, and *GATA6* expression does not disappear (Kuijk et al., 2012).

To investigate whether inhibition of ROCK could help to balance the potential negative effects of PD0325901, we included the combination of three inhibitors, '3i' (PD0325901 + CHIR99021 + Y27632) targeting MEK/ERK, GSK3 $\beta$  and ROCK signalling pathways. Y27632 has also been used to culture hESC and hiPSC in suspension (Zweigerdt et al., 2011). Another inhibitor, A83-01, is an inhibitor of the TGF $\beta$  receptor upstream of Activin A/Nodal. TGF $\beta$  receptor activity is needed to maintain primed EpiSC. All four inhibitors are collectively termed YPAC when used together. In our experiments, we termed this combination '4i'. To recognize the integrity of the cells and their organelles in the embryo disc of 6-day-old rabbit embryos cultured under 2i, 3i and 4i conditions, we performed transmission electron microscopy analysis. Investigating the effect of the inhibitors on the cellular ultrastructure of the embryo revealed afflicted mitochondria, ER and GC, while the volume of vacuoles as well as residual and ABs increased



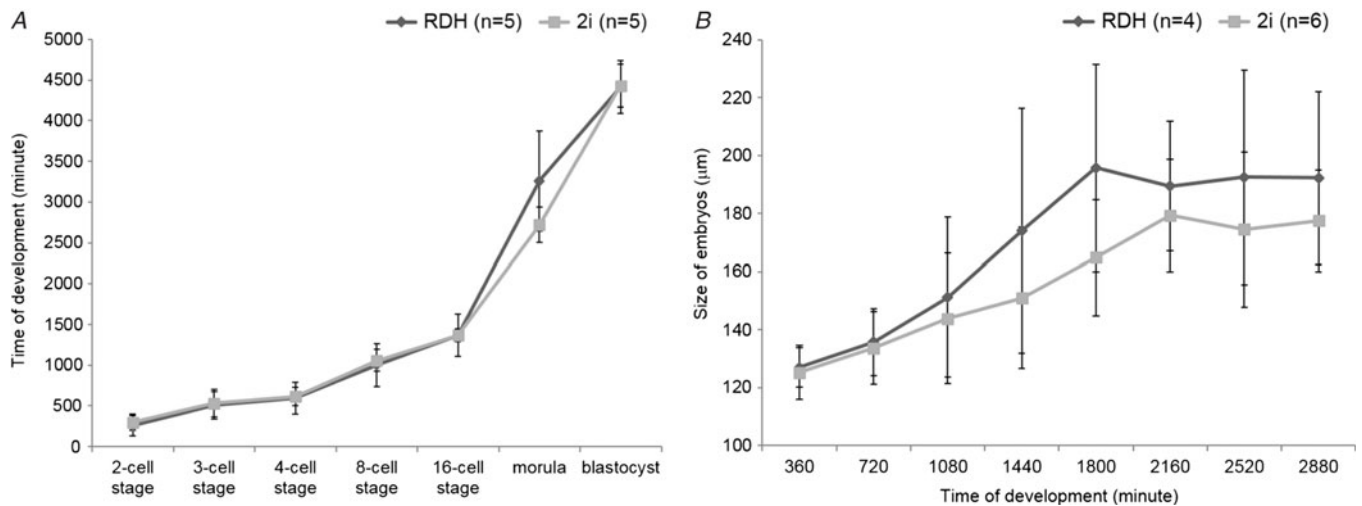


**Figure 3.** Tracking of embryonic development under control culture conditions (RDH) against 2i-supplemented culture medium using time-lapse video technology. (A) Measuring the time between the different embryonic developmental stages, from the 2-cell stage up to the early blastocyst stage (75 h). (B) Measuring the time from the morula stage up to the blastocyst stage over the span of 48 h. Embryos cultured in 2i condition displayed slightly faster development and a smaller size compared with the control embryos in RDH;  $n$  = number of investigated embryos.

in 4i- and 3i-treated embryos. Despite ROCK inhibition by means of Y27632 in 4i formulation, the relative volume of ABs was not reduced. Treatment with 2i did not result in significant disturbance of the organelles. Treatment with 2i maintained the integrity of mitochondria, ER and GC in ICM cells of rabbit embryos while maintaining the volumes of the structures, indicating minimum damage.

In conclusion, regarding inhibition, the factors involved in Ras–MEK–ERK, GSK3 $\beta$  and TGF $\beta$  signalling pathways have been implicated to alter the ratio of OCT4-positive epiblasts and GATA6-positive hypoblasts. As a result of MEK inhibition, the number of hypoblast cells reduced in mouse and rat embryos, but in human, porcine and bovine embryos the numbers of hypoblast cells were only moderately reduced, suggesting that hypoblast formation is FGF independent. Our results demonstrated that rabbit embryos respond in a similar way to non-rodent embryos, because the hypoblast still forms even under combined MEK and GSK3 $\beta$  inhibition.

**Financial support.** This work was supported by the Slovak Research and Development Agency (grant numbers APVV-14-0043 and APVV-17-0124); by the Scientific Grant Agency (grant numbers VEGA 1/0049/19 and VEGA 1/0160/18) and Cultural and Educational Grant Agency of the Ministry of Education, Science, Research and Sport of the Slovak Republic and the Slovak Academy of Sciences (grant number KEGA 026SPU-4/2018); by Hungarian Research and Development Agency (grant numbers MFB-00130-00131/2010, ANR-NKTH/09-GENM-010-01 and OTKA-K77913); by European Cooperation in Science and Technology (COST) Action (Rabbit Genome Biology; RGB) (grant number TD1101) and COST Action (Sharing Advances on Large Animal Models) (SALLAM) (grant number BM1308).

**Conflicts of interest.** None.

**Ethical standards.** All experiments and studies were conducted in accordance with recommendations described in the Hungarian Code of Practice for the Care and Use of Animals for Scientific Purposes and the experiments were approved by the Hungarian Animal Care and Ethics Committee (approval number; 767/001/2003). No human subjects, human data or human material were used in this study.

**Supplementary material.** To view supplementary material for this article, please visit <https://doi.org/10.1017/S0967199419000753>

## References

- Bain J, Plater L, Elliott M, Shpiro N, Hastie CJ, McLauchlan H, Klevernic I, Arthur JS, Alessi DR and Cohen P (2007) The selectivity of protein kinase inhibitors: a further update. *Biochem J* **408**, 297–315.
- Besenfelder U, Modl J, Muller M and Brem G (1997) Endoscopic embryo collection and embryo transfer into the oviduct and the uterus of pigs. *Theriogenology* **47**, 1051–60.
- Bolender RP and Weibel ER (1973) A morphometric study of the removal of phenobarbital-induced membranes from hepatocytes after cessation of treatment. *J Cell Biol* **56**, 746–61.
- Bosze Z, Hiripi L, Carnwath JW and Niemann H (2003) The transgenic rabbit as model for human diseases and as a source of biologically active recombinant proteins. *Transgenic Res* **12**, 541–53.
- Brons IG, Smithers LE, Trotter MW, Rugg-Gunn P, Sun B, Chuva de Sousa Lopes SM, Howlett SK, Clarkson A, Ahrlund-Richter L, Pedersen RA and Vallier L (2007) Derivation of pluripotent epiblast stem cells from mammalian embryos. *Nature* **448**, 191–5.
- Buehr M, Meek S, Blair K, Yang J, Ure J, Silva J, McLay R, Hall J, Ying QL and Smith A (2008) Capture of authentic embryonic stem cells from rat blastocysts. *Cell* **135**, 1287–98.
- du Puy L, Lopes SM, Haagsman HP and Roelen BA (2011) Analysis of co-expression of OCT4, NANOG and SOX2 in pluripotent cells of the porcine embryo, *in vivo* and *in vitro*. *Theriogenology* **75**, 513–26.
- Fang ZF, Gai H, Huang YZ, Li SG, Chen XJ, Shi JJ, Wu L, Liu A, Xu P and Sheng HZ (2006) Rabbit embryonic stem cell lines derived from fertilized, parthenogenetic or somatic cell nuclear transfer embryos. *Exp Cell Res* **312**, 3669–82.
- Hao J, Li TG, Qi X, Zhao DF and Zhao GQ (2006) WNT/beta-catenin pathway up-regulates Stat3 and converges on LIF to prevent differentiation of mouse embryonic stem cells. *Dev Biol* **290**, 81–91.
- Harris D, Huang B and Oback B (2013) Inhibition of MAP2K and GSK3 signaling promotes bovine blastocyst development and epiblast-associated expression of pluripotency factors. *Biol Reprod* **88**, 74.
- Haura EB, Ricart AD, Larson TG, Stella PJ, Bazhenova L, Miller VA, Cohen RB, Eisenberg PD, Selaru P, Wilner KD and Gadgeel SM (2010) A phase II study of PD-0325901, an oral MEK inhibitor, in previously treated patients with advanced non-small cell lung cancer. *Clin Cancer Res* **16**, 2450–7.
- Honda A, Hirose M, Inoue K, Ogonuki N, Miki H, Shimozawa N, Hatori M, Shimizu N, Murata T, Hirose M, Katayama K, Wakisaka N, Miyoshi H, Yokoyama KK, Sankai T and Ogura A (2008) Stable embryonic stem cell lines in rabbits: potential small animal models for human research. *Reprod Biomed Online* **17**, 706–15.

- Honda A, Hirose M and Ogura A (2009) Basic FGF and Activin/Nodal but not LIF signaling sustain undifferentiated status of rabbit embryonic stem cells. *Exp Cell Res* **315**, 2033–42.
- Ivics Z, Hiripi L, Hoffmann OI, Mátés L, Yau TY, Bashir S, Zidek V, Landa V, Geurts A, Pravenec M, Rüllicke T, Bösze Z and Izsvák Z (2014) Germline transgenesis in rabbits by pronuclear microinjection of Sleeping Beauty transposons. *Nat Protoc* **9**, 794–809.
- Jin DI, Kim DK, Im KS and Choi WS (2000) Successful pregnancy after transfer of rabbit blastocysts grown *in vitro* from single-cell zygotes. *Theriogenology* **54**, 1109–16.
- Kawamata M and Ochiya T (2010) Generation of genetically modified rats from embryonic stem cells. *Proc Natl Acad Sci USA* **107**, 14223–8.
- Kuijk EW, van Tol LT, Van de Velde H, Wubbolts R, Welling M, Geijssen N and Roelen BA (2012) The roles of FGF and MAP kinase signaling in the segregation of the epiblast and hypoblast cell lineages in bovine and human embryos. *Development* **139**, 871–82.
- Liskovych M, Chuykin I, Ranjan A, Safina D, Popova E, Tolkunova E, Mosienko V, Minina JM, Zhdanova NS, Mullins JJ, Bader M, Alenina N and Tomilin A (2011) Derivation, characterization, and stable transfection of induced pluripotent stem cells from Fischer344 rats. *PLoS One* **6**, e27345.
- Lorusso PM, Adjei AA, Varterasian M, Gadgeel S, Reid J, Mitchell DY, Hanson L, DeLuca P, Bruzek L, Piens J, Asbury P, Van Becelaere K, Herrera R, Sebolt-Leopold J and Meyer MB (2005) Phase I and pharmacodynamic study of the oral MEK inhibitor CI-1040 in patients with advanced malignancies. *J Clin Oncol* **23**, 5281–93.
- Maraghechi P, Hiripi L, Toth G, Bontovics B, Bosze Z and Gócza E (2013) Discovery of pluripotency-associated microRNAs in rabbit preimplantation embryos and embryonic stem-like cells. *Reproduction* **145**, 421–37.
- Men H and Bryda EC (2013) Derivation of a germline competent transgenic Fischer 344 embryonic stem cell line. *PLoS One* **8**, e56518.
- Nichols J and Smith A (2011) The origin and identity of embryonic stem cells. *Development* **138**, 3–8.
- Nichols J, Silva J, Roode M and Smith A (2009) Suppression of Erk signalling promotes ground state pluripotency in the mouse embryo. *Development* **136**, 3215–22.
- Osteil P, Taponnier Y, Markossian S, Godet M, Schmaltz-Panneau B, Jouneau L, Cabau C, Joly T, Blachère T, Gócza E, Bernat A, Yerle M, Acloque H, Hidot S, Bosze Z, Duranthon V, Savatier P and Afanassieff M (2013) Induced pluripotent stem cells derived from rabbits exhibit some characteristics of naive pluripotency. *Biol Open* **2**, 613–28.
- Piliszek A, Madeja ZE and Plusa B (2017) Suppression of ERK signalling abolishes primitive endoderm formation but does not promote pluripotency in rabbit embryo. *Development* **144**, 3719–30.
- Plusa B, Piliszek A, Frankenberg S, Artus J and Hadjantonakis AK (2008) Distinct sequential cell behaviours direct primitive endoderm formation in the mouse blastocyst. *Development* **135**, 3081–91.
- Puschel B, Bitzer E and Viebahn C (2010) Live rabbit embryo culture. *Cold Spring Harb Protoc* **2010**, pdb.prot5352.
- Qi X, Li TG, Hao J, Hu J, Wang J, Simmons H, Miura S, Mishina Y and Zhao GQ (2004) BMP4 supports self-renewal of embryonic stem cells by inhibiting mitogen-activated protein kinase pathways. *Proc Natl Acad Sci USA* **101**, 6027–32.
- Rathjen J, Lake JA, Bettess MD, Washington JM, Chapman G and Rathjen PD (1999) Formation of a primitive ectoderm like cell population, EPL cells, from ES cells in response to biologically derived factors. *J Cell Sci* **112**, 601–12.
- Rodriguez A, Allegrucci C and Alberio R (2012) Modulation of pluripotency in the porcine embryo and iPS cells. *PLoS One* **7**, e49079.
- Roode M, Blair K, Snell P, Elder K, Marchant S, Smith A and Nichols J (2012) Human hypoblast formation is not dependent on FGF signalling. *Dev Biol* **361**, 358–63.
- Sato N, Meijer L, Skaltsounis L, Greengard P and Brivanlou AH (2004) Maintenance of pluripotency in human and mouse embryonic stem cells through activation of Wnt signaling by a pharmacological GSK-3-specific inhibitor. *Nat Med* **10**, 55–63.
- Savatier P, Osteil P and Tam PP (2017) Pluripotency of embryo-derived stem cells from rodents, lagomorphs, and primates: slippery slope, terrace and cliff. *Stem Cell Res* **19**, 104–12.
- Schmaltz-Panneau B, Jouneau L, Osteil P, Taponnier Y, Afanassieff M, Moroldo M, Jouneau A, Daniel N, Archilla C, Savatier P and Duranthon V (2014) Contrasting transcriptome landscapes of rabbit pluripotent stem cells *in vitro* and *in vivo*. *Anim Reprod Sci* **149**, 67–79.
- Shen MM and Leder P (1992) Leukemia inhibitory factor is expressed by the preimplantation uterus and selectively blocks primitive ectoderm formation *in vitro*. *Proc Natl Acad Sci USA* **89**, 8240–4.
- Sheth PR, Liu Y, Hesson T, Zhao J, Vilenchik L, Liu YH, Mayhood TW and Le HV (2011) Fully activated MEK1 exhibits compromised affinity for binding of allosteric inhibitors U0126 and PD0325901. *Biochemistry* **50**, 7964–76.
- Taponnier Y, Afanassieff M, Aksoy I, Aubry M, Moulin A, Medjani L, Bouchereau W, Mayère C, Osteil P, Nurse-Francis J, Oikonomakos I, Joly T, Jouneau L, Archilla C, Schmaltz-Panneau B, Peynot N, Barasc H, Pinton A, Lecardonnell J, Gócza E, Beaujean N, Duranthon V and Savatier P (2017) Reprogramming of rabbit induced pluripotent stem cells toward epiblast and chimeric competency using Kruppel-like factors. *Stem Cell Res* **24**, 106–17.
- Tesar PJ, Chenoweth JG, Brook FA, Davies TJ, Evans EP, Mack DL, Gardner RL and McKay RD (2007) New cell lines from mouse epiblast share defining features with human embryonic stem cells. *Nature* **448**, 196–9.
- Thisse B and Thisse C (2005) Functions and regulations of fibroblast growth factor signaling during embryonic development. *Dev Biol* **287**, 390–402.
- Thomson JA, Kalishman J, Golos TG, Durning M, Harris CP, Becker RA and Hearn JP (1995) Isolation of a primate embryonic stem cell line. *Proc Natl Acad Sci USA* **92**, 7844–8.
- Thomson JA, Itskovitz-Eldor J, Shapiro SS, Waknitz MA, Swiergiel JJ, Marshall VS and Jones JM (1998) Embryonic stem cell lines derived from human blastocysts. *Science* **282**, 1145–7.
- Vallier L, Alexander M and Pedersen RA (2005) Activin/Nodal and FGF pathways cooperate to maintain pluripotency of human embryonic stem cells. *J Cell Sci* **118**, 4495–509.
- Wang S, Tang X, Niu Y, Chen H, Li B, Li T, Zhang X, Hu Z, Zhou Q and Ji W (2007) Generation and characterization of rabbit embryonic stem cells. *Stem Cells* **25**, 481–9.
- Watanabe K, Ueno M, Kamiya D, Nishiyama A, Matsumura M, Wataya T, Takahashi JB, Nishikawa S, Nishikawa S, Muguruma K and Sasai Y (2007) A ROCK inhibitor permits survival of dissociated human embryonic stem cells. *Nat Biotechnol* **25**, 681–6.
- Xu RH, Chen X, Li DS, Li R, Addicks GC, Glennon C, Zwaka TP and Thomson JA (2002) BMP4 initiates human embryonic stem cell differentiation to trophoblast. *Nat Biotechnol* **20**, 1261–4.
- Xu RH, Peck RM, Li DS, Feng X, Ludwig T and Thomson JA (2005) Basic FGF and suppression of BMP signaling sustain undifferentiated proliferation of human ES cells. *Nat Methods* **2**, 185–90.
- Ying QL, Wray J, Nichols J, Battle-Morera L, Doble B, Woodgett J, Cohen P and Smith A (2008) The ground state of embryonic stem cell self-renewal. *Nature* **453**, 519–23.
- Zweigerdt R, Olmer R, Singh H, Haverich A and Martin U (2011) Scalable expansion of human pluripotent stem cells in suspension culture. *Nat Protoc* **6**, 689–700.